



Comprehensive analysis of HOXC8 associated with tumor microenvironment characteristics in colorectal cancer

Sifan Wu^{a,b,1}, Dandan Zhu^{b,1}, Huolun Feng^{a,c,1}, Yafang Li^d, Jianlong Zhou^c,
Yong Li^{a,c,g,**}, Tiejing Hou^{a,b,e,f,*}

^a School of Medicine, South China University of Technology, Guangzhou, Guangdong, 510006, China

^b Guangdong Center for Clinical Laboratory, Guangdong Provincial People's Hospital (Guangdong Academy of Medical Sciences), Southern Medical University, Guangzhou, Guangdong, 510080, China

^c Department of Gastrointestinal Surgery, Department of General Surgery, Guangdong Provincial People's Hospital (Guangdong Academy of Medical Sciences), Southern Medical University, Guangzhou, Guangdong, 510080, China

^d The First Affiliated Hospital of Xiamen University (Tongan Branch), The Third Hospital of Xiamen, Xiamen, Fujian, 316000, China

^e Hospital Office, Huazhong University of Science and Technology Union Shenzhen Hospital/Shenzhen Nanshan People's Hospital, Shenzhen, Guangdong, 518052, China

^f Shenzhen University Medical School, Shenzhen, Guangdong, 518073, China

^g Department of Gastrointestinal Surgery, Ganzhou Municipal Hospital, Ganzhou, China

ARTICLE INFO

Keywords:

Colorectal cancer
HOXC8
Prognosis
Epithelial-mesenchymal transition
Tumor microenvironment

ABSTRACT

Background: Accumulating evidence have highlighted the essential roles of HOX genes in embryonic development and carcinogenesis. As a member of the HOX gene family, the abnormal expression of *HOXC8* gene is associated with the progression and metastasis of various tumors. However, potential roles of *HOXC8* in colorectal cancer (CRC) prognosis and tumor microenvironment (TME) remodeling remain unclear.

Methods: We conducted an integrated analysis of clinical and molecular characteristics, relevant oncogenic and immune regulation roles and drug sensitivity features of *HOXC8* in CRC.

Results: *HOXC8* expression was markedly high expressed in CRC samples compared to normal samples, and the upregulated expression of *HOXC8* was associated with poor prognosis. High *HOXC8* expression was significantly associated with invasion-related pathways especially epithelial-mesenchymal transition (EMT). In vitro experiments showed significantly up-regulated *HOXC8* expression in some CRC cell lines and its promoting effect on EMT and cell proliferation. TME categorization through transcriptomic analysis of CRC patients with high *HOXC8* expression identified two different TME subtypes known as immune-enriched with fibrotic subtype and immune-depleted subtype. Patients with immune-enriched, fibrotic subtype exhibited significantly longer progression-free survival (PFS), upregulated PD-L1 and CTLA4 expression and higher TMB than those with the immune-depleted subtype.

Conclusions: *HOXC8* overexpression was associated with poor prognosis and specific TME subtypes in CRC. This study provided valuable resource for further exploring the potential mechanisms and therapeutic targets of HOX genes in CRC.

* Corresponding author. School of Medicine, South China University of Technology, Guangzhou, Guangdong, 510006, China.

** Corresponding author. School of Medicine, South China University of Technology, Guangzhou, Guangdong, 510006, China.

E-mail addresses: liyong@gdph.org.cn (Y. Li), sz_houtiejing@yeah.net (T. Hou).

¹ These authors contributed equally to this work.

1. Introduction

Colorectal cancer (CRC) ranks the third predominant cause of malignancy mortality worldwide, surpassing 1.85 million cases and 0.85 million deaths per year [1]. Recently, the comprehensive therapy for colorectal cancer has been further explored, and combination treatment with the targeted drug is the major treatment strategy for patients with metastatic CRC [2]. Despite the continuous development of medication regimen, it remains difficult to achieve breakthroughs in the treatment of metastatic patients [3]. Thus, there is an urgent need to explore effective molecular targets against CRC.

Homeobox (HOX) genes are a subgroup of highly conserved homeobox superfamily consisting of 39 transcription factors classified into four clusters (HOXA, HOXB, HOXC, HOXD), which obviously affect a variety of cellular processes, including apoptosis, proliferation, cell shape, cell migration and angiogenesis [4,5]. Accumulating evidence has highlighted the potential role of HOX genes in the progression and metastasis of several tumors, as well as in resistance to treatment [6,7]. Aberrant HOX genes has been frequently discovered in various primary tumors, mainly manifested as altered expression following epigenetic changes including variations in methylation profiles of histone modifications and promoters, less commonly as gene mutations, translocation and amplification [8,9]. Furthermore, DNA methylation of HOX genes is closely relevant to specific tumor cell types and molecular subtypes [10]. As a member of the HOX family, *HOXC8* can modulate genes associate with proliferation, adhesion and migration and be regarded as a global regulator for the growth and differentiation of human cell [11]. It has been reported that *HOXC8* participates in the growth and migration of breast cancer cell by promoting the epithelial-mesenchymal transition (EMT) of tumor cells [12]. Additionally, up-regulated *HOXC8* expression was also observed in prostate cancer, cervical cancer and lung cancer and facilitated the metastasis and progression of tumor cells [13–15].

Previous studies have shown that multiple types of immune cell within the tumor microenvironment (TME) can influence the progression and metastasis of tumor cell [16,17]. However, potential roles of *HOXC8* in CRC prognosis and TME remodeling remain unclear. In this study, we conducted an integrated analysis of clinical and molecular characteristics, relevant oncogenic and immune regulation roles and drug sensitivity features of *HOXC8* in CRC. The in vitro experiments showed significantly up-regulated *HOXC8* expression in some CRC cell lines and its promoting effect on EMT and cell proliferation. In addition, the expression patterns based on 29 functional gene expression signatures (Fges) were applied to thoroughly depict the TME in subgroup with increased *HOXC8* expression. These results may provide valuable resource for further exploring the potential mechanisms and therapeutic targets of HOX genes in CRC.

2. Materials and method

2.1. Data preparation

Transcriptome RNA-seq profiles and clinical annotation of colorectal cancer(CRC) were obtained from The Cancer Genome Atlas (TCGA) database (<https://portal.gdc.cancer.gov>). Patients receiving pharmaceutical therapy were included for subsequent analyses.

2.2. *HOXC8* expression among clinical features in CRC

The expression level of *HOXC8* between normal and tumor tissues were analyzed for CRC patients via using the package “limma” of R. Then we selected patients receiving pharmaceutical therapy for follow-up analysis. Furthermore, we categorized patients to analyze *HOXC8* expression on the basis of other clinical traits including age, gender, pathological stage and survival status.

2.3. Estimation of immunological characteristics

The single sample gene set enrichment analysis (ssGSEA) was applied to assess the abundance of infiltrating cells of stroma and immune via utilizing the package gene set variation analysis (GSVA) of R [18]. The datasets for immune-correlated genes, representing a series of immune checkpoints, immune cell subpopulations, human leukocyte antigen (HLA) and immune-associated functions, were retrieved from the previous studies [19,20]. The total infiltration for immune or stromal cells in tumor microenvironment (TME) was evaluated with ESTIMATE algorithm based on mRNA expression profiles [21]. The proportions of infiltrating fibroblasts and endothelial cells in CRC tissues were estimated based on xCell deconvolution algorithm [22].

2.4. Functional enrichment analysis

To uncover the distinctions in biological pathways between high-*HOXC8* and low-*HOXC8* subgroups, the Gene set variation analysis (GSVA) package was applied to quantify the activity of pathway via calculating the pathway enrichment scores (PES) for each sample [18]. The gene set “c2.cp.kegg.v7.4.symbols.gmt” of GSVA analysis were downloaded from the MSigDB database.

2.5. Unsupervised clustering analysis

To further estimate the specific signatures of the TME in the subgroup of *HOXC8* expression, we calculated intensity scores of the functional gene expression signatures (Fges) by in-house R package “GSVA” implementation of the ssGSEA based on the Fges in the

previously published literature [23] which can describe the TME cell phenotype and states, and the processes of physiological and pathological signaling. Unsupervised dense Leuven clustering was applied to identify different TME expression patterns on the basis of the intensity scores for 29 Fges [24]. The optimal weight threshold of clustering was determined according to Silhouette scores, Calinski Harabasz and David Bolduin index.

2.6. Analysis of the mutational landscape in CRC

Somatic mutation files from the TCGA database were acquired using the package “TCGAbiolinks” and visualized via the function of oncoplot from “maftool” package [25,26]. The mutation load for each sample was measured by the function of tmb.

2.7. OncoPredict for the analysis of drug sensitivity

Genomics of Drug Sensitivity in Cancer (GDSC) dataset (<https://www.cancerrxgene.org/>) includes the drug sensitivity information of tumor cells and molecular markers for drug response. The package “OncoPredict” of R [27] associates the profile of tissues gene expression with the half maximal inhibitory concentration (IC50) to drugs for the tumor cell lines from GDSC database to predict drug responses in vivo for tumor patients. After the drugs were calculated, unpaired t-tests was applied to estimate the drug sensitivity between the high-HOXC8 and low-HOXC8 subgroups.

2.8. Cell culture

CRC cell lines RKO, SW480, and human colon epithelial cell line NCM460 were purchased from ATCC (American Type Culture Collection, Manassas, VA, USA). All cell lines were cultured in DMEM medium containing 10 % fetal bovine serum (FBS, Gibco-BRL, Paisley, UK) under standard culture conditions (37 °C, 5 % CO₂).

2.9. RNA extraction and quantitative real-time PCR (qRT-PCR)

The Trizol extraction kit (Invitrogen, Carlsbad, CA, USA) was employed to extract total RNA of cell lines. The transcription of RNA into cDNA was completed with PrimeScript RT Master Mix (Takara, China) and SYBR® qPCR Master Mix (Vazyme, China) was then applied to perform qRT-PCR. The Δ Cq method was used to calculate the relative expression for each sample. The primer sequences were provided in Supplemental files 1 (Table S1).

2.10. HOXC8 siRNA transfection of SW480 cells

SW480 cells were seeded into the six-well plates overnight to grow into a monolayer. The transfection solution consisting of negative control siRNA (RiboBio, Guangzhou) or three distinct HOXC8 siRNAs and transfection reagent (Invitrogen) were supplemented to 2 ml medium per well. After 48 h, the cells were treated with trypsin and applied for subsequent analysis.

2.11. Western blot analysis

Extraction of proteins was conducted by using radioimmunoprecipitation assay (RIPA) lysis buffer (Beyotime Institute of Biotechnology). The proteins from samples were separated by SDS-PAGE and transferred to polyvinylidene difluoride (PVDF) membrane. After transferring, the PVDF membrane was incubated with primary antibodies overnight at 4 °C. After washing with 1 × TBS/0.1 % Tween-20, the membrane was incubated with the secondary antibody (1 h, room temperature). LI-COR Odyssey Infrared Imaging System was applied to acquire images. The corresponding antibodies include Anti-HOXC8 antibody (15448-1-AP, ProteinTech Group), anti-E-cadherin antibody (ab231303, Abcam), anti-Vimentin antibody (ab16700, Abcam), Anti-Cyclin D1 antibody (26939-1-AP, ProteinTech Group) and β -actin (BM0627, Boster).

2.12. Statistical analysis

Use the normality test to analyze whether the quantitative data conforms to the normal distribution. When the sample size is greater than 50, use the Kolmogorov-Smirnov test, otherwise use the Shapiro-Wilk test. The test result P value > 0.05 indicates that the data is considered normally distributed. Missing data were imputed by utilizing modified non-responder imputation (mNRI) for categorical variables and multiple imputation (MI) for continuous variables. Univariate outliers identification via Tukey’s box-plot method and bivariate outliers detection via Mahalanobis distance method followed by outlier removal. Statistical significance of quantitative data was analyzed utilizing Student’s t-test for normally distributed variables and the Wilcoxon test for nonnormally distributed variables. For survival analyses, the approaches of Kaplan-Meier and log-rank test were used to obtain survival curves while estimated the statistical significance. According to the optimal cut-off value of HOXC8 analyzed by the package “survival” of R, samples in TCGA-CRC were divided into high and low HOXC8 expression subgroups. Correlation analysis was conducted adopting the Spearman correlation test. All tests were two-sided and the threshold for statistical significance was set at p-value < 0.05. All data processing was performed using R 4.1.3 software.

3. Results

3.1. Prognostic value of *HOXC8* and its correlation with clinical features in CRC

Fig. 1 presents the workflow of our study. We compared the expression of *HOXC8* in CRC samples and normal samples from TCGA database and found that *HOXC8* was high expressed in CRC samples (Fig. S1A). Kaplan-Meier analysis further uncovered that the patients with high *HOXC8* expression was obviously related to poor prognosis in CRC (Fig. 2A). Furthermore, we investigated the association between *HOXC8* expression and clinical characteristics (Fig. S1B). Detailed basic clinicopathological characteristics along with treatment-related variables of all cases in High-*HOXC8* and Low-*HOXC8* subgroups are exhibited in Table 1. Univariate and multivariate cox analyses disclosed that the expression level of *HOXC8* served as an independent predictor for the prognosis of CRC patients (Fig. 2B and C). These data displayed the close relevance of *HOXC8* with clinical features such as N stage, T stage and pathological stage, implying its potential role in cancer progression and prognosis, possibly serving as a significant prognostic biomarker.

Previous studies illuminated that overexpression of HOX genes may confer therapy resistance by enhancing epidermal growth factor receptor (EGFR) expression and signaling in cancer cells [9,28]. Therefore, we assessed the association of *HOXC8* expression with drug sensitivity (Fig. 2D). As a result, the subpopulation with decreased expression of *HOXC8* exhibited higher sensitivity to AMG-319 (targeting drug, PI3K inhibitor), AZ960 (targeting drug, JAK inhibitor), Foretinib (targeting drug, VEGFR inhibitor), JAK 8517 (targeting drug, JAK inhibitor), JQ1 (targeting drug, BET inhibitor), Mitoxantrone (targeting drug, topoisomerase II inhibitor), Niraparib (targeting drug, PARP inhibitor), Olaparib (targeting drug, PARP inhibitor), Teniposide (targeting drug, topoisomerase II inhibitor), XAV939 (targeting drug, TNKS inhibitor) and ZM447439 (targeting drug, Aurora inhibitor), which were considered as drug candidates for the therapy of patients with reduced *HOXC8* expression in CRC.

3.2. *HOXC8*-related biological characteristics and its association with EMT processes

To understand the biological behaviors associated with these distinct *HOXC8* expression subpopulations, we employed GSEA enrichment analysis (Fig. 3A, Table S2). Subpopulation with high *HOXC8* expression was remarkably enriched in invasion-related pathways including epithelial mesenchymal transition (EMT), transforming growth factor beta (TGF- β), cell adhesion, angiogenesis, WNT and calcium regulation signaling pathways, indicating poor survival outcomes for subgroups with high *HOXC8* expression. Furthermore, immune response-associated processes such as type 2 immune response, activation of monocytes, macrophages and B cells, MHC class II biosynthesis and complement receptor-mediated signaling pathways were significantly upregulated in high *HOXC8*

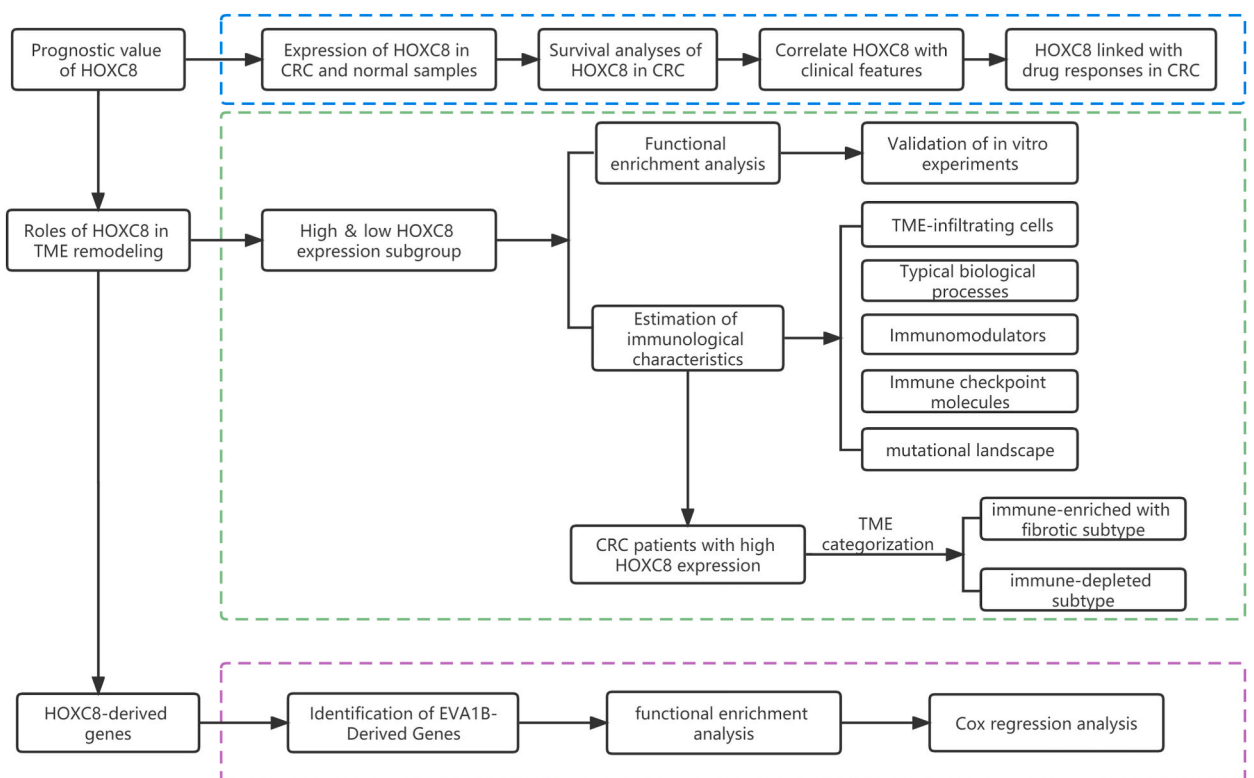


Fig. 1. The workflow of this study.

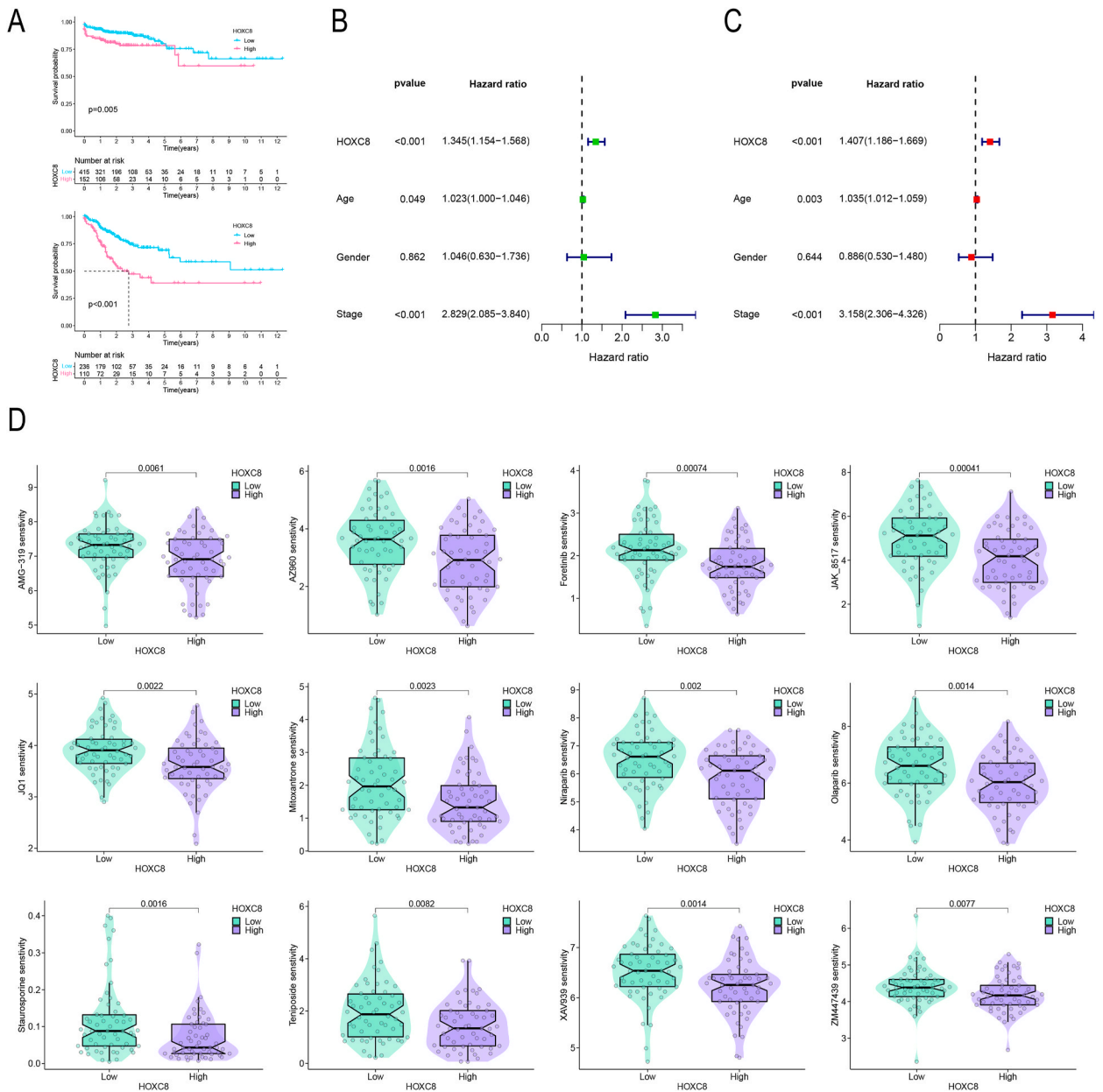


Fig. 2. Prognostic value of HOXC8 and its correlation with clinical features in colorectal cancer (CRC). (A) Kaplan–Meier curves of overall survival (OS) (top) and progression-free survival (PFS) (bottom) for patients with high and low HOXC8 expression in The Cancer Genome Atlas (TCGA) cohort. (B, C) Uni- and multivariate Cox analyses are performed to reveal the interrelations of clinical features and HOXC8 expression with the survival outcomes of CRC. Hazard ratio <1 indicated protective factors for survival and hazard ratio >1 indicated risk factors for survival. (D) The sensitivity of different drug between the high-HOXC8 and low-HOXC8 subgroups. High HOXC8 expression subgroups, purple; Low HOXC8 expression subgroups, green.

expression subgroup. Previous reports have demonstrated that CD8⁺ T cell exclusion occurred primarily in patients with collagen- and fibroblast-rich tumors, and that activated fibroblasts producing excess TGF-β and extracellular matrix (ECM) with rearrangement of collagen fiber can impede the immune infiltration of CD8⁺ and CD4⁺ T cells into the core of tumor [29–31]. Additionally, intrinsic factors of tumor cell can also obstruct immune cell infiltration, such as WNT/β-catenin pathway activation impairing the production of chemokine as well as CD103+ cDC1 recruitment [32,33]. Thus, we speculated that upregulated HOXC8 might result in the activation of tumor escape-related pathways, thereby suppressing the migration and infiltration of anti-tumor immune cells into the tumor parenchyma. To further explore such correlations between HOXC8 and tumor escape-related pathways at the molecular level, we focused on analyzing the transcriptional levels of genes associated with EMT processes in different HOXC8 expression subgroups (Fig. 3B, Table S3). Heatmap displayed that the expression of genes involved in EMT processes was generally upregulated in the

Table 1
Basic clinicopathological characteristics along with treatment-related variables in High-HOXC8 and Low-HOXC8 subgroups.

| Characteristics | High HOXC8 n = 152 | Low HOXC8 n = 415 |
|-------------------------------|--------------------|-------------------|
| Age at diagnosis | | |
| ≤65 | 64(42.1) | 189(45.5) |
| >65 | 88(57.9) | 226(54.5) |
| Gender | | |
| Male | 79(51.9) | 220(53.0) |
| Female | 73(48.1) | 196(47.0) |
| MSI status | | |
| MSI-H | 50(32.9) | 23(5.5) |
| MSI-L | 15(9.9) | 48(11.6) |
| MSS | 58(38.1) | 184(44.3) |
| Unknown | 29(19.1) | 160(38.6) |
| Pathologic T | | |
| T1 | 2(1.3) | 16(3.9) |
| T2 | 14(9.2) | 87(21.0) |
| T3 | 111(73.0) | 279(67.2) |
| T4 | 25(16.5) | 32(7.7) |
| Unknown | 0(0) | 1(0.2) |
| Pathologic N | | |
| N0 | 87(57.2) | 242(58.3) |
| N1 | 29(19.1) | 106(25.6) |
| N2 | 35(23.0) | 66(15.9) |
| Unknown | 1(0.7) | 1(0.2) |
| Pathologic M | | |
| M0 | 113(74.3) | 323(77.8) |
| M1 | 19(12.5) | 47(11.3) |
| Unknown | 20(13.2) | 45(10.9) |
| Pathologic stage | | |
| I | 16(10.5) | 85(20.5) |
| II | 69(45.4) | 144(34.7) |
| III | 44(29.0) | 125(30.1) |
| IV | 19(12.5) | 48(11.6) |
| Unknown | 4(2.6) | 13(3.1) |
| Radiation Therapy | | |
| Yes | 1(0.6) | 13(3.1) |
| No | 53(34.9) | 166(40) |
| Unknown | 98(64.5) | 236(56.9) |
| Pharmaceutical Therapy | | |
| Yes | 35(23.0) | 80(19.3) |
| No | 44(28.9) | 97(23.4) |
| Unknown | 73(48.1) | 238(57.3) |

MSI, microsatellite instability; MSS, microsatellite stability; T, tumor; N, lymph node; M, metastasis.

subgroup with elevated *HOXC8* expression, further supporting our speculation. Interestingly, we found that the expression of the epidermal growth factor (EGF)-like molecule, amphiregulin (AREG), one of the genes relevant to EMT, exhibited a strong negative correlation with the expression of *HOXC8* (Fig. 3B and C). Further analysis indicated that patients with high *AREG* expression were significantly correlated with good prognosis (Fig. 3D). Although *AREG* was initially regarded as an epithelial- and mesenchymal-derived factor, several studies have shown that *AREG* can be produced by a variety of activated immune cell populations including basophils, mast cells, CD4⁺ T cells and group 2 innate lymphoid cells (ILC2) in various inflammatory conditions, which may be a crucial element for type 2 immune response-mediated tolerance and resistance [34]. Therefore, it is not surprising that the prognostic protective role of *AREG* in CRC contrasted with prior reports in other tumor types where prognostic risk factors were observed [35,36]. Besides, *HOXC8* expression was analyzed in several CRC cell lines (RKO, SW480) based on qRT-PCR. The expression level of *HOXC8* was obviously upregulated in CRC cell lines compared with a human normal colonic epithelial cell line (NCM460) (Fig. 3E). To further confirm the connection of *HOXC8* expression with EMT and cell proliferation, we detected the abundance of cell proliferation-related protein (Cyclin D1) and EMT-related proteins including the interstitial marker (Vimentin) and the epithelial markers (E-cadherin) through western blotting. The results indicated that knockdown of *HOXC8* in SW480 cells promoted the expression of E-cadherin and inhibited the expression of vimentin and Cyclin D1.

The above results indicated that the expression of *HOXC8* not only affects the progression and prognosis of CRC by mediating the upregulation of tumor escape-related pathways such as EMT, but also may be involved in immune regulation within the TME.

3.3. Immune landscape of different *HOXC8* expression subpopulations

Tumor are encompassed by a dynamic microenvironment composed of multiple infiltrating immune cells. Interactions between tumor cells and immune components can affect tumor immunogenicity and the response to immune checkpoint blockade (ICB) [37].

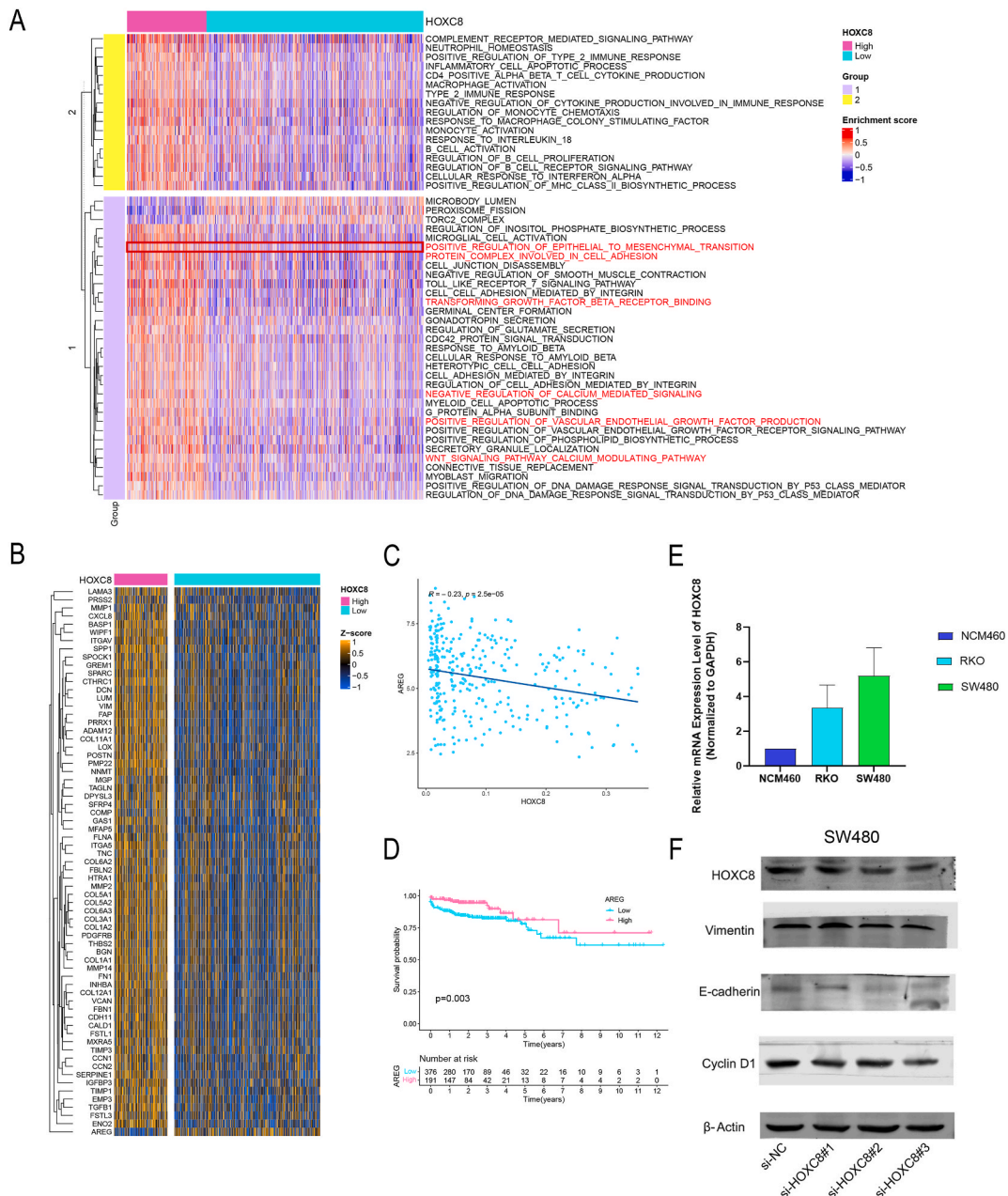


Fig. 3. HOXC8-related biological characteristics and its association with epithelial-mesenchymal transition (EMT) processes. (A) Heatmap presenting the biological process distinctions in *HOXC8* expression subgroups. Red indicated activated pathways and blue indicated inhibited pathways. Group 1 represented non-immune response related pathways and group 2 represented immune response related pathways. Invasion-related processes were marked in red font. The process highlighted by the red box was the positive regulation of EMT. (B) Heatmap displaying mRNA relative Z-score abundance of genes related to EMT in different *HOXC8* expression subgroups. Blue represented low expression and orange represented high expression. (C) Correlation of amphiregulin (AREG) expression with *HOXC8* expression. (D) Kaplan–Meier curves of OS for patients with high and low AREG expression in CRC. (E) *HOXC8* mRNA expression in different colon cancer cell lines. (F) Detection of EMT-related proteins Vimentin and E-cadherin, and proliferation-related protein Cyclin D1 after treatment with siRNA directed against *HOXC8* in SW480 cells. The original images from Western blot were accessible in supplementary file 1.

Considering the distinction of the enrichment of immune-related pathways and prognostic characteristics between high and low *HOXC8* expression subgroups, we subsequently explored the specific relation between *HOXC8* expression and immune cell infiltration. Antitumor lymphocyte cell subpopulations (natural killer cells, effector memory CD4+/CD8+ T cells) and immunosuppressive cells (myeloid derived suppressor cells (MDSCs), regulatory T (Treg) cells and M2-like macrophages) were significantly elevated in high *HOXC8* expression subgroup (Fig. 4A, Table S4, Table S5). Previous studies have demonstrated that most solid tumors exhibited three

major immune phenotypes, known as immune exclusion, immune inflammation and immune desert, primarily stratified by inflammation levels of TME [38,39]. Although the high *HOXC8* expression subgroup was characterized by high levels of immune cell infiltration, the prognosis of this *HOXC8* subgrouping displayed poor; therefore, the specific signatures of the TME in subgroup with elevated *HOXC8* expression needed to be further estimated. The expression patterns based on 29 functional gene expression signatures (Fges) covering the majority of functional components and stromal, immune, and other cell populations from the tumor were applied to thoroughly depict the TME in subgroup with increased *HOXC8* expression according to published literature [23]. Pearson correlation analysis on 29 Fges was employed to uncover two major groups showing positively correlated (co-activated or co-inhibited) across the corresponding dataset (Fig. 4B, Table S6). One group composed of Fges defining T cell populations involved in regulatory T cell (Treg), T-helper 1 (Th1) subtypes and effector T cell, as well as macrophage, NK cell, checkpoint inhibition and MHC class II expression. Taken together, these Fges comprised the immune compartment for TME, encompassing anti-tumor and tumor-promoting immune processes. The second group included Fges related to stromal components such as matrix, matrix remodeling and cancer-associated fibroblasts (CAFs), as well as angiogenesis, endothelium, and tumor-promoting cytokine expression.

To classify the TME of the patients with up-regulated *HOXC8* expression applying the curated list of 29 Fges, unsupervised dense Louvain clustering of their ssGSEA scores was employed to assess the expression patterns [24]. The results showed that the molecular profiles of CRC with high *HOXC8* expression could be divided into two distinct microenvironments known as immune-enriched with fibrotic subtype and immune-depleted subtype (Fig. 4C, Table S7). Further analysis of the differences between these two subgroups with high *HOXC8* expression in overall survival (OS) and progression-free survival (PFS) indicated that the patients with immune-enriched, fibrotic subtype had significantly longer PFS than those with the immune-depleted subtype (Fig. 4D).

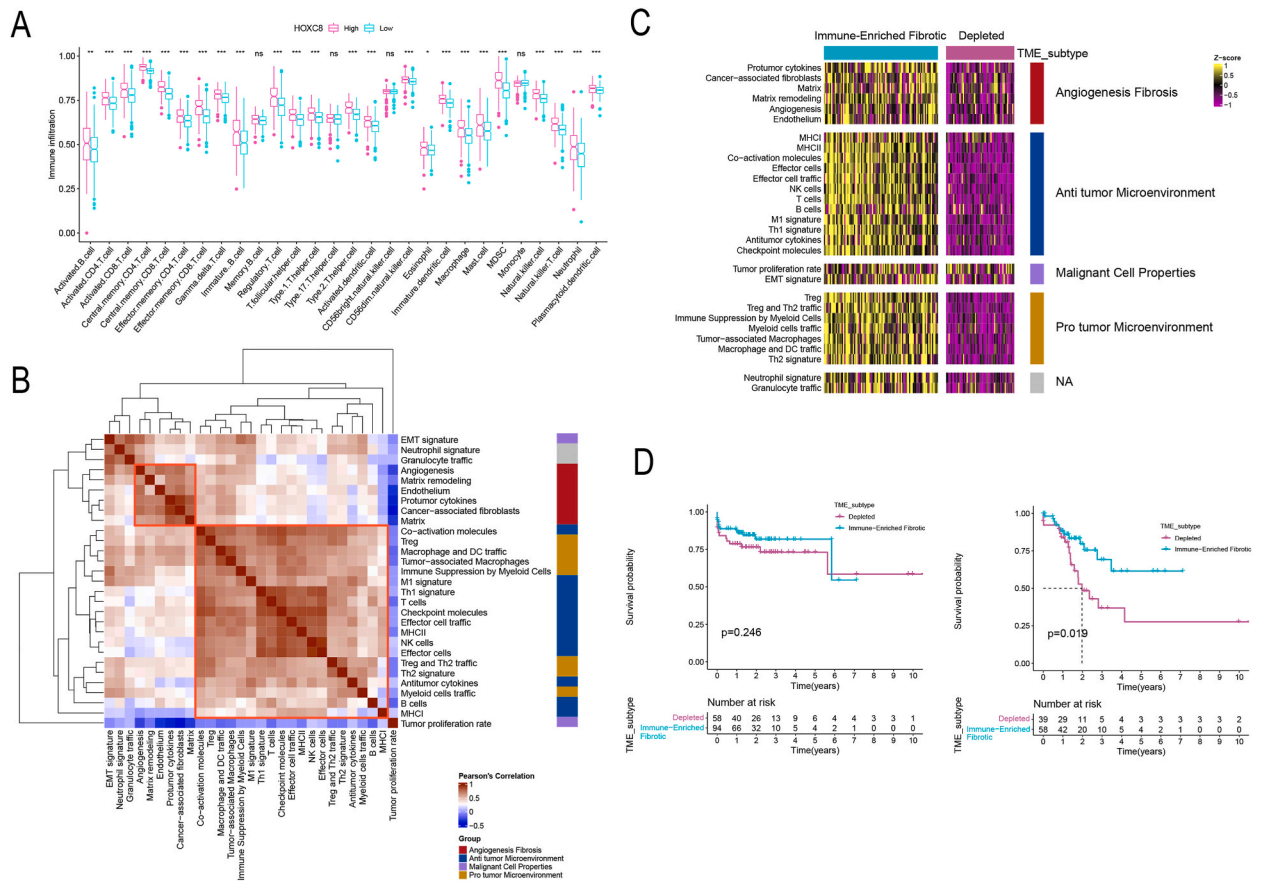


Fig. 4. Immune landscape of different *HOXC8* expression subpopulations. (A) The abundance of tumor-infiltrating immune cells in subgroups with high and low *HOXC8* expression. Lines, boxes, and whiskers represent medians, 25%–75 %, and 5%–95 % percentiles, respectively. Not significant (n.s.), * $P < 0.05$, ** $P < 0.01$, *** $P < 0.001$. (B) Pearson correlation between the scores of 29 functional gene expression signatures (Fges) of CRC samples. Positive and negative associations are marked in red and blue, respectively. (C) Heatmap of CRC patients with high *HOXC8* expression divided into two different TME subtypes by unsupervised dense clustering based on 29 Fges. Yellow indicated up-regulated gene signature scores, purple indicated down-regulated gene signature scores. (D) OS (left) and PFS (right) survival curves of tumor microenvironment (TME) subtypes in high *HOXC8* expression subpopulation.

3.4. Immune microenvironment characteristics associated with HOXC8

Given the distinction of tumor-infiltrating immune cells in the two HOXC8 subgroups, we then explore the features of the TME connected with HOXC8 expression. High HOXC8 expression associated with increased immune and stromal scores as well as diminished tumor purity (Fig. 5A), suggesting the up-regulation of stromal and immune cells within the TME of patients with high HOXC8

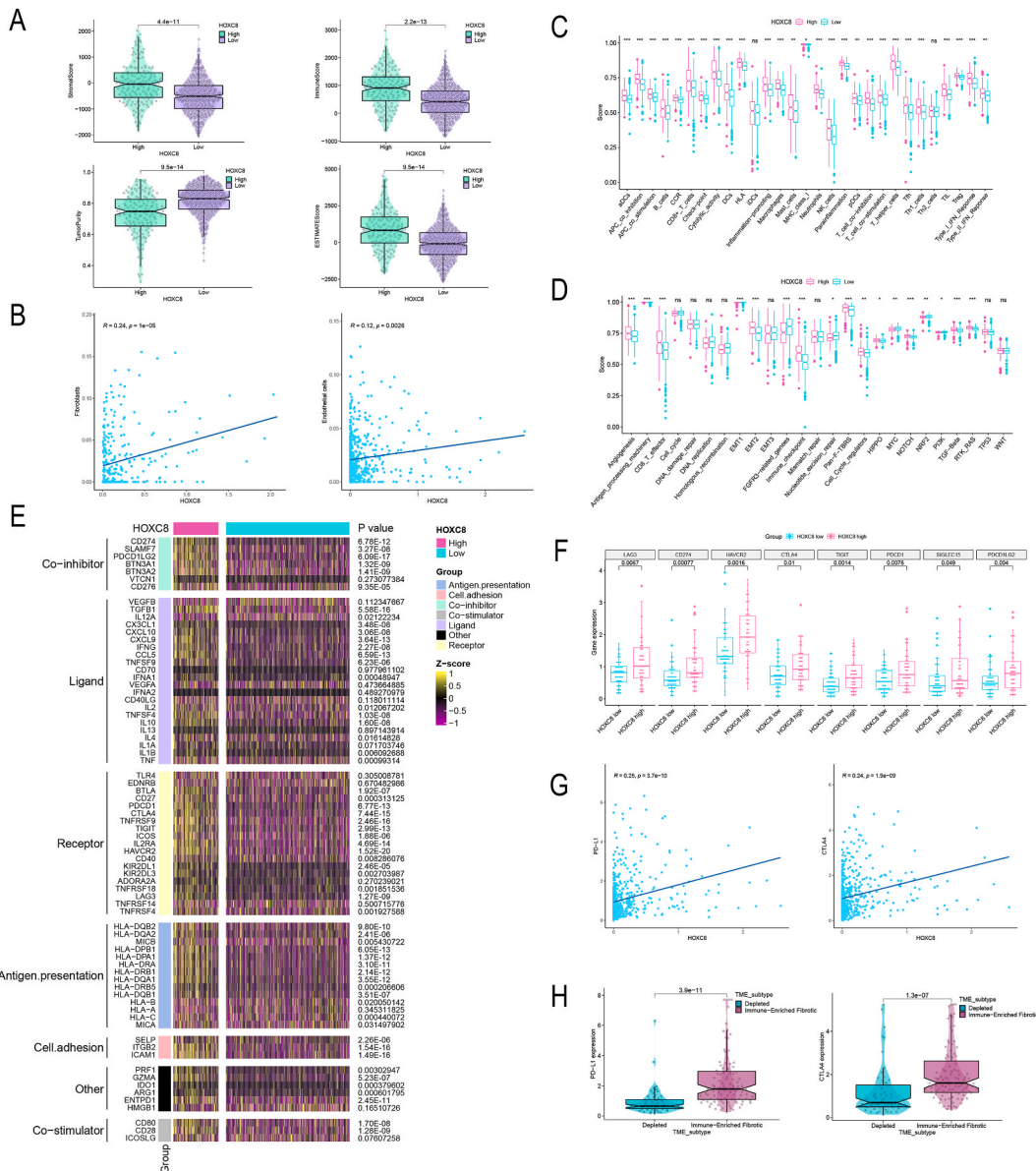


Fig. 5. Immune microenvironment characteristics associated with HOXC8. (A) Estimation of the distinction in stromal and immune score, tumor purity and estimate score in low and high HOXC8 expression subgroups. High HOXC8 expression subgroups, green; Low HOXC8 expression subgroups, purple. (B) Correlation of HOXC8 expression with the proportions of infiltrating fibroblasts (left) and endothelial cells (right). (C) Differences in the enrichment of immune signatures between subpopulations with low and high HOXC8 expression. Lines, boxes, and whiskers represent medians, 25%–75 %, and 5%–95 % percentiles, respectively. Not significant (n.s.), *P < 0.05, **P < 0.01, ***P < 0.001. (D) Comparing the enrichment of representative biological processes in HOXC8 expression subgroups. Lines, boxes, and whiskers represent medians, 25%–75 %, and 5%–95 % percentiles, respectively. Not significant (n.s.), *P < 0.05, **P < 0.01, ***P < 0.001. (E) Heatmap of immunomodulators abundance between HOXC8 expression subgroups. Purple represented low expression and yellow represented high expression. (F) Difference in immune checkpoint molecules expression between HOXC8 low expression and high expression subpopulations. Lines, boxes, and whiskers represent medians, 25%–75 %, and 5%–95 % percentiles, respectively. (G) Correlation of HOXC8 expression with programmed cell death 1 ligand (PD-L1) (left) and cytotoxic T-lymphocyte-associated protein 4(CTLA4) (right) expression. (H) Difference in PD-L1 (left) and CTLA4 (right) expression in TME subtypes with high HOXC8 expression.

expression. Furthermore, we found that the expression level of *HOXC8* exhibited a strong positive correlation with the abundance of fibroblasts and endothelial cells evaluated by xCell analysis (Fig. 5B). These results provided further support for the existence of an immune-enriched, fibrotic subtype of TME in patients with high *HOXC8* expression. Subsequent analyses showed that both anti-tumor and pro-tumor immune signatures were obviously elevated in the high *HOXC8* expression subgroup, accompanied by significantly activated nucleotide excision repair-related pathways as well as stromal activation processes consisting of EMT, FGFR3-related genes, angiogenesis and pan-fibroblast TGF- β response signature (pan-F-TBRs) (Fig. 5C and D).

Immunomodulators (IMs) play crucial roles in cancer immunotherapy through involvement in shaping the TME, and their multiple agonists and antagonists have begun to be assessed in clinical oncology [40]. To further estimate the potential effects of *HOXC8* on the TME in CRC patients, it is essential to investigate the expression levels of IMs in different *HOXC8* expression subpopulations. The abundance of IMs varied across the *HOXC8* expression subpopulations and we found that most IMs were significantly upregulated in the high-*HOXC8* expression subgroup, especially the immune inhibitor PD-L1 and the immune activators CD28 and TNFRSF9, consistent with the result that high *HOXC8* expression subgroup displayed the TME subtype with immune activation and immunosuppression (Figs. 4C and 5E, Table S8).

To further reveal the roles of *HOXC8* in the immune regulation within the TME, we analyzed the mRNA abundance of immune checkpoint-associated genes characterizing *HOXC8* expression subpopulations (Fig. 5F). We noted that the raised expression of *HOXC8* led to the comprehensively up-regulation of the expression of immune checkpoint molecules, such as PD-L1 and CTLA4 molecules. Correlation analysis further confirmed that tumors with elevated expression of *HOXC8* were obviously related to higher expression level of PD-L1 and CTLA4 (Fig. 5G). Furthermore, we analyzed the expression of PD-L1 and CTLA4 in two TME subtypes of the subpopulation with high *HOXC8* expression. The results presented that patients with immune-enriched fibrosis subtype exhibited significantly upregulated expression of PD-L1 and CTLA4 compared to patients with the immune-depleted subtype (Fig. 5H), suggesting a potential response to PD-1/L1 blockade therapy.

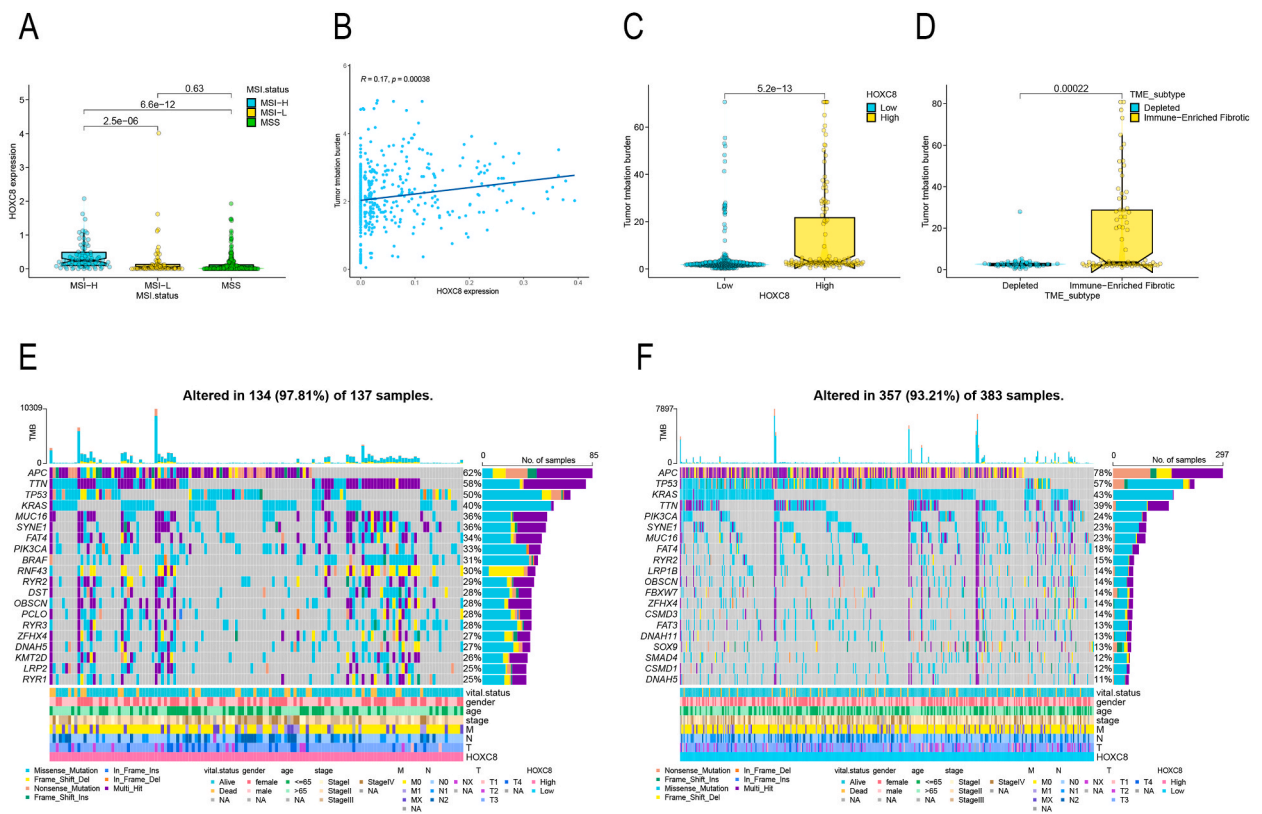
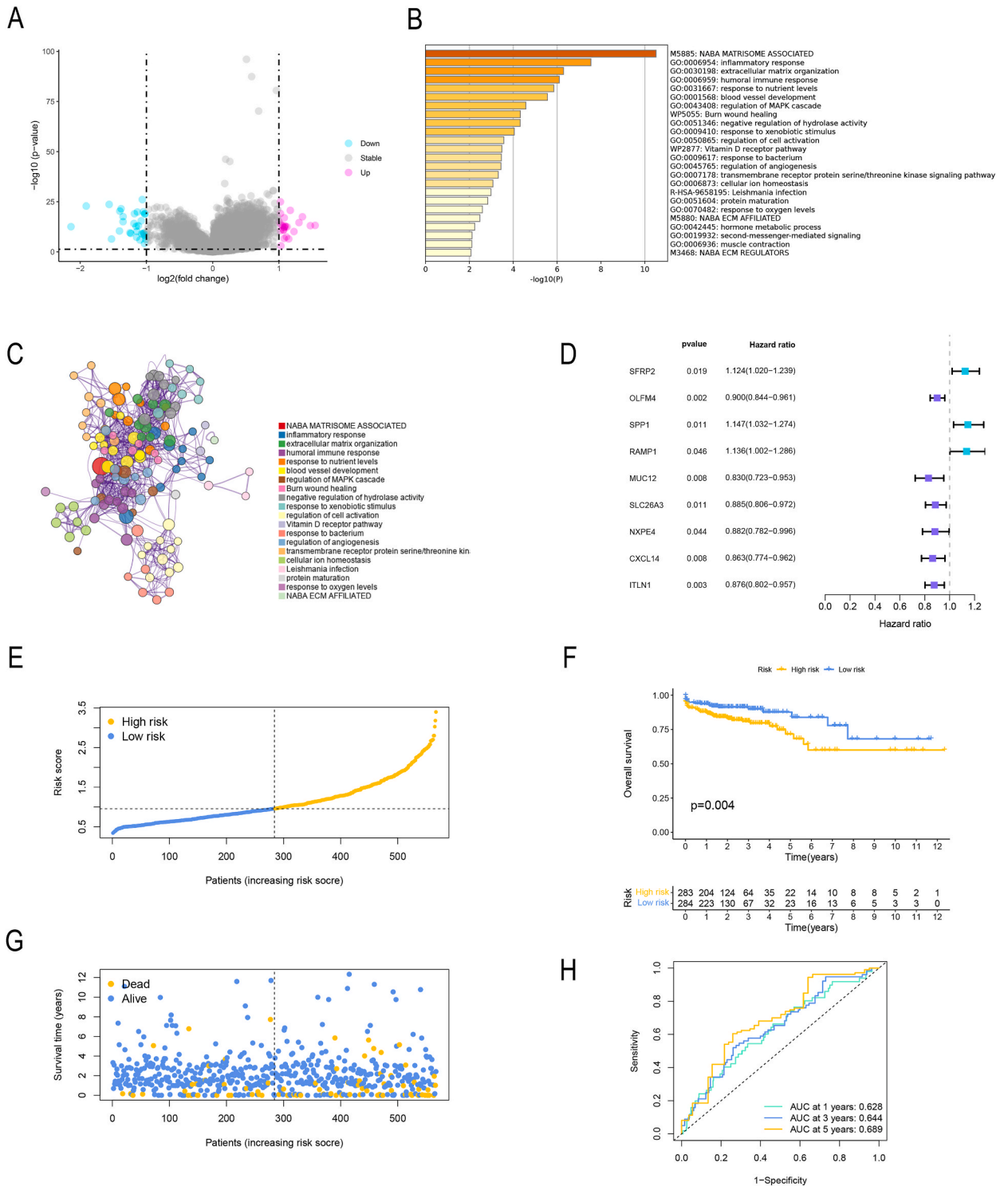


Fig. 6. Somatic mutations in *HOXC8* subtypes. (A) Differences in *HOXC8* expression among subpopulations with different microsatellite instability (MSI) status. (B) Correlation plots displaying associations between *HOXC8* expression and tumor mutation burden (TMB). (C) Differences in TMB between *HOXC8* expression subgroups. (D) Differences in TMB between TME subtypes with high *HOXC8* expression. (E–F) Waterfall plot exhibiting obviously mutated genes in CRC samples of the high and low *HOXC8* expression subpopulations. Mutated genes sorted by mutation rate (rows, top 20). Individual patients are represented in each column. The top bar plot presents the TMB. The right bar plot displays the mutation frequency of each gene in different *HOXC8* expression subgroups. Age, sex, vital status, T, N, M and stage are displayed as annotations of CRC patients. T, tumor; N, lymph node; M, metastasis.



(caption on next page)

Fig. 7. Identification of *HOXC8*-derived genes and their functional enrichment analysis. (A) Volcano plot presenting the downregulated and upregulated genes in CRC samples between high and low *HOXC8* expression subgroups. Pink dots represented up-regulated genes, gray dots represented nonsignificant genes, and blue dots represented down-regulated genes. (B) GO enrichment analysis of *HOXC8*-derived genes based on Metascape platform. (C) Interaction network of enriched pathways for *HOXC8*-derived genes. (D) Prognostic analyses of *HOXC8*-derived genes for the CRC cohorts by applying univariate Cox regression model. Hazard ratio <1 indicated protective factors for survival and hazard ratio >1 indicated risk factors for survival. (E) Distribution of low-risk and high-risk CRC subgroups and the means of *HOXC8*-derived risk scores (dashed vertical lines). (F) Kaplan–Meier curves of OS for low-risk and high-risk CRC subgroups. (G) Individual survival status of two CRC subgroups. (H) The ROC curve of 1-, 3-, and 5-year OS predictions in CRC patients by the multivariable Cox regression model.

3.5. Immunophenoscore and somatic mutations in *HOXC8* subtypes

Although cancer treatment has been revolutionized by immune checkpoint inhibition, durable responses have not been observed in the majority of patients [41]. Earlier identification of responders could improve clinical prognosis and is urgently needed. Therefore, we investigated the potential value of immune checkpoint inhibitors, such as CTLA-4/PD-1 inhibitors, in immune checkpoint blockade (ICB) therapy in CRC patients with different *HOXC8* expression though employing the immunotherapy score. The CRC patients in the different *HOXC8* expression subgroups illustrated obvious distinctions in PD-1-negative and CTLA4-negative immunotherapy scores (Fig. S1C). Of note, the immunotherapy score of CTLA4 varied across *HOXC8* subgroups, with lower efficacy observed in the high *HOXC8* expression subgroup than that in the low *HOXC8* expression subgroup (Fig. S1D). Furthermore, the MSI-H subgroup was markedly correlated to elevated expression of *HOXC8* compared to the MSI-L and MSS subgroups (Fig. 6A).

Accumulating evidence suggests that somatic mutations observed in the cancer genomes are associated with responsiveness to immunotherapy. Thus, we explored the link between *HOXC8* expression and tumor mutation burden (TMB). Correlation analysis of *HOXC8* expression and TMB showed that the increased expression of *HOXC8* was markedly connected with higher TMB (Fig. 6B). Further analysis indicated that the high *HOXC8* expression subgroup correlated with poor clinical outcome displayed a higher TMB frequency (Fig. 6C), consistent with a previous clinical report that high TMB may serve as a poor prognostic factor in cancer patients [42]. By comparing the frequency of TMB in different TME subtypes of CRC patients with high *HOXC8* expression, we observed that tumors with an immune-enriched, fibrotic subtype exhibited higher TMB (Fig. 6D).

Next, we estimated the significantly mutated genes (SMGs) in the distinct *HOXC8* subgroups. The landscapes of SMG illustrated that the subpopulation with high *HOXC8* expression showed more extensive TMB than the subpopulation with low *HOXC8* expression. For instance, *TTN*, the 2nd most significantly mutated gene, occurred at rates of 58 % versus 39 % in the high and low *HOXC8* expression subgroups, respectively (Fig. 6E and F). Interestingly, *APC* (62 % vs. 78 %) presented lower somatic mutation rates in the subgroup with high *HOXC8* expression. These data contribute to a better understanding of the connection of *HOXC8* expression with somatic TMB and susceptibility or resistance to immunity therapy mediated by genetic alterations.

3.6. Identification of *HOXC8*-derived genes and their functional enrichment analysis

By comparing the differences of gene expression between the high and low *HOXC8* expression subgroups (Fig. 7A), we identified 55 *HOXC8*-derived genes in CRC patients based on the cutoffs of adjusted p-value <0.05 and |fold-change| >1. Subsequently, Metascape was employed to predict the pathway enrichment and biological functions of 55 *HOXC8*-derived genes based on GO approaches (Fig. 7B). The associations between the pathways were visualized by network connection diagrams (Fig. 7C). These results presented that the most of biological functions and processes were associate with tumor escape and inflammatory immune response. A total of 9 *HOXC8*-derived genes were significantly associated with the prognosis of CRC patients using univariate cox regression models (Fig. 7D). Based on multivariate-Cox stepwise regression analysis for the expression of 9 *HOXC8*-derived genes, we established a multivariable Cox regression model and the formula was as follows: risk score = $(-0.059672101) * OLFM4$ expression + $0.110238509 * SPP1$ expression + $(-0.088417417) * ITLN1$ expression. According to the mean value, we divided patients with CRC into low-risk and high-risk subgroups (Fig. 7E). Survival analysis indicated that patients in low-risk subpopulation were significantly correlated with good prognosis (Fig. 7F). However, there was no significant distinction in survival status between the low-risk and high-risk subgroups (Fig. 7G). The predictive advantage accessed by using ROC curves was particularly reflected in 5-years survival (Fig. 7H). The above analyses showed that the interactions between *HOXC8*-derived genes play essential roles in CRC progression, ultimately affecting the prognosis of patients.

4. Discussion

Previous studies have highlighted the essential roles of HOX genes in embryonic development and carcinogenesis [4]. While several studies have associated aberrant expression of the *HOXC8* gene with various tumor metastasis-related biological pathways [12,43–45], few studies have comprehensively explored the potential roles of *HOXC8* in CRC patients based on the analysis of TME signatures. In this study, we conducted an integrated analysis of clinical and molecular characteristics, relevant oncogenic and immune regulation roles and drug sensitivity features of *HOXC8* in CRC. This research may provide a valuable resource for further exploration of the underlying value of HOX genes in oncology.

Based on RNA-sequencing data, we found that the expression of *HOXC8* was significantly elevated in CRC samples compared with normal tissues. Importantly, the upregulated *HOXC8* expression was associated with undesirable clinical outcomes of patients with CRC, consistent with previous reports [15,45]. Our further analysis presented the close relevance of *HOXC8* with clinical features such

as N stage, T stage and pathological stage, implying its potential role in cancer progression and prognosis, possibly serving as a significant prognostic biomarker.

The onset and progression of tumor stems from the accumulation of molecular signatures enabling cancer cells to survive, proliferate and escape from immune surveillance, while cultivating their ability to adapt to hostile environments [46]. The effective targeted therapies against these molecular traits are critical for individual patients with CRC. Consistent with previous studies [47,48], analyzing the association of *HOXC8* expression with drug sensitivity found lower sensitivity to most chemotherapy agents in the subpopulation with elevated *HOXC8* expression, providing clues to clarify the poor survival outcomes of the high *HOXC8* expression subgroup.

To understand the biological behaviors associated with distinct *HOXC8* expression subpopulations, we employed GSVA enrichment analysis. Subpopulation with high *HOXC8* expression was remarkably enriched in invasion-related pathways, consistent with previous reports that the mRNA of *HOXC8* may serve as a potential indicator of tumor invasion and metastasis [12,44,49,50]. Interestingly, our study showed that immune response-associated processes were also significantly upregulated in high *HOXC8* expression subgroup. Previous reports have demonstrated that CD8⁺ T cell exclusion occurred primarily in patients with collagen- and fibroblast-rich tumors, and that activated fibroblasts producing excess TGF- β and ECM with rearrangement of collagen fiber can impede the immune infiltration of CD8⁺ and CD4⁺ T cells into the core of tumor [29–31]. Additionally, intrinsic factors of tumor cell can also obstruct immune cell infiltration, such as WNT/ β -catenin pathway activation impairing the production of chemokine as well as CD103+ cDC1 recruitment [32,33]. Thus, we speculated that upregulated *HOXC8* might result in the activation of tumor escape-related pathways, thereby suppressing the migration and infiltration of anti-tumor immune cells into the tumor parenchyma. To further explore such correlations between *HOXC8* and tumor escape-related pathways at the molecular level, we focused on analyzing the transcriptional levels of genes associated with EMT processes in different *HOXC8* expression subgroups. The results presented that the expression of genes involved in EMT processes was generally upregulated in the subgroup with elevated *HOXC8* expression, further supporting our speculation. In the present study, the expression level of *HOXC8* was obviously upregulated in several CRC cell lines. More importantly, we further confirmed the promoting effect of *HOXC8* expression on EMT and cell proliferation by western blotting. The above results indicated that the expression of *HOXC8* not only affects the progression and prognosis of CRC by mediating the upregulation of tumor escape-related pathways such as EMT, but also may be involved in immune regulation within the TME.

Given the distinction of the enrichment of immune-related pathways and prognostic characteristics between high and low *HOXC8* expression subgroups, we subsequently explored the specific relation between *HOXC8* expression and immune cell infiltration. Antitumor lymphocyte cell subpopulations and immunosuppressive cells were significantly elevated in high *HOXC8* expression subgroup. Although the high *HOXC8* expression subgroup was characterized by high levels of immune cell infiltration, the prognosis of this *HOXC8* subgrouping displayed poor; therefore, according to published literature [23], we applied the expression patterns based on 29 Fges covering the majority of functional components and stromal, immune, and other cell populations from the tumor to thoroughly depict the TME in subgroup with increased *HOXC8* expression and then two distinct microenvironments known as immune-enriched with fibrotic subtype and immune-depleted subtype were identified in high *HOXC8* expression subgroup. Further analysis of the differences between these two subgroups with high *HOXC8* expression in OS and PFS indicated that the patients with immune-enriched, fibrotic subtype had significantly longer PFS than those with the immune-depleted subtype, the comparison of the survival curves between these two subtypes was generally consistent with the results of the previous study [23]. Besides, high *HOXC8* expression associated with increased immune and stromal scores as well as diminished tumor purity, suggesting the up-regulation of stromal and immune cells within the TME of patients with high *HOXC8* expression. These results provided further support for the existence of an immune-enriched, fibrotic subtype of TME in patients with high *HOXC8* expression.

To further reveal the roles of *HOXC8* in the immune regulation within the TME, we analyzed the mRNA abundance of IMs and immune checkpoint-associated genes characterizing *HOXC8* expression subpopulations. We found that most IMs were significantly upregulated in the high-*HOXC8* expression subgroup, especially the immune inhibitor PD-L1 and the immune activators CD28 and TNFRSF9, consistent with the result that high *HOXC8* expression subgroup displayed the TME subtype with immune activation and immunosuppression. Furthermore, we noted that the raised expression of *HOXC8* led to the comprehensively up-regulation of the expression of immune checkpoint molecules, such as PD-L1 and CTLA4 molecules. Subsequently, we analyzed the expression of PD-L1 and CTLA4 in two TME subtypes of the subpopulation with high *HOXC8* expression. The results presented that patients with immune-enriched fibrosis subtype exhibited significantly upregulated expression of PD-L1 and CTLA4 compared to patients with the immune-depleted subtype, suggesting a potential response to PD-1/L1 blockade therapy.

We further investigated the potential value of immune checkpoint inhibitors, such as CTLA-4/PD-1 inhibitors, in ICB therapy in CRC patients with different *HOXC8* expression though employing the immunotherapy score. The CRC patients in the different *HOXC8* expression subgroups illustrated obvious distinctions in PD-1-negative and CTLA4-negative immunotherapy scores. Of note, the immunotherapy score of CTLA4 varied across *HOXC8* subgroups, with lower efficacy observed in the high *HOXC8* expression subgroup than that in the low *HOXC8* expression subgroup. Accumulating evidence suggests that somatic mutations observed in the cancer genomes are associated with responsiveness to immunotherapy. The results showed that the high *HOXC8* expression subgroup correlated with poor clinical outcome displayed a higher TMB frequency, consistent with a previous clinical report that high TMB may serve as a poor prognostic factor in cancer patients [42]. Furthermore, we observed that tumors with an immune-enriched, fibrotic subtype exhibited higher TMB in CRC patients with high *HOXC8* expression. Carbone et al. demonstrated that tumors with elevated TMB and PD-L1 expression showed a higher response to immune checkpoint inhibitors compared to those harboring only one of these factors [51], further illustrating that patients with the immune-enriched, fibrosis subtype in the high *HOXC8* expression subgroup may benefit the most from immunotherapy.

We further identified 55 *HOXC8*-derived genes in CRC patients that were mostly associate with tumor escape and inflammatory

immune response, indicative of their essential roles in the progression of CRC. Based on multivariable Cox regression analysis, we established a HOXC8-derived genomic model. Thereafter, ROC curves presented that the HOXC8-derived genomic model displayed favorable efficiency in predicting 5-year OS probabilities of CRC patients. The above analyses showed that the interactions between HOXC8-derived genes may play indispensable roles in CRC progression, ultimately affecting the prognosis of patients.

In this study, we performed a comprehensive analysis of the clinical and molecular features, related oncogenic and immunomodulatory roles of HOXC8 in colorectal cancer. Our study found that significantly up-regulated HOXC8 expression in CRC cell lines and its promoting effect on EMT and cell proliferation, as well as its association with poor prognosis. Furthermore, two distinct TME subtypes were identified in the subgroup with increased HOXC8 expression: an immune-enriched with fibrotic subtype and an immune-depleted subtype. Therefore, our study can provide valuable resource for further exploring the potential mechanisms and therapeutic targets of HOX genes in CRC. However, there are still several limitations in our study. First, due to technical limitations, we analyzed the infiltration of immune cells within the TME based on algorithms. Second, in this study, we found that the immune-enriched fibrotic subtype of TME existed in patients with high HOXC8 expression, which remains to be experimentally verified. Third, part of the analysis in this study was based on public databases, lacking our own clinical cohort to verify the correlation between HOXC8 and tumor immune landscape, as well as its prognostic value in CRC. However, we conducted several *in vitro* experiments to affirm the biological function of HOXC8, which made up for the lack of verification of database mining to a certain extent. Thus, further exploration based on large clinical cohorts is needed in the future.

5. Conclusion

In summary, the integrated analysis of clinical and molecular characteristics, relevant oncogenic and immune regulation roles and drug sensitivity features of HOXC8 in CRC identified the potential roles of HOXC8 in CRC prognosis and TME remodeling that were not fully investigated by previous analysis. Our findings may open new paths for further exploring the potential mechanisms and therapeutic targets of HOX genes in CRC.

Funding statement

This work was supported by the National Natural Science Foundation of China, China (82002508, 31970696, and 81502975), the Excellent Young Talent Program of Guangdong Provincial People's Hospital, China (KY012021186), Guangdong Provincial People's Hospital supporting Funding for NSFC Program (KY012021159), Guangdong Medical Scientific Research Foundation (B2022168), the Natural Science Foundation of Guangdong Province, China (2020A1515010136), Outstanding Young Medical Talents in Guangdong Province of Guangdong Provincial People's Hospital, Individualized precision therapy for adenocarcinoma of esophagogastric junction, China (KJ012019439), Asymmetric Wound Antimicrobial Dressing Based on Functional Bacterial Cellulose (20200202004), National key Clinical Specialty Construction Project (2021–2024, No. 2022YW030009), and KEO12021230. The contents of this work were not influenced by the sponsoring foundations.

Data availability statement

The datasets used and analyzed for this study were obtained from The Cancer Genome Atlas (TCGA) database (<https://portal.gdc.cancer.gov>).

Ethics approval and consent to participate

The retrospective study protocol was reviewed and approved by the Guangdong Provincial People's Hospital, Guangdong Academy of Medical Sciences Research Ethics Committee. All patients signed the preoperative informed consent, and after patients' identification information was removed, a waiver of informed consent was obtained. All procedures performed in the studies involving human participants were in accordance with the ethical standards of the institutional and/or national research committee and with the 1964 Helsinki declaration and its later amendments or comparable ethical standards.

Consent for publication

Not applicable.

CRedit authorship contribution statement

Sifan Wu: Conceptualization, Data curation, Formal analysis, Methodology, Software, Validation, Visualization, Writing – original draft. **Dandan Zhu:** Data curation, Formal analysis, Software, Validation, Writing – original draft. **Huolun Feng:** Conceptualization, Formal analysis, Methodology, Software, Supervision, Writing – review & editing. **Yafang Li:** Data curation, Methodology, Software, Investigation. **Jianlong Zhou:** Project administration, Visualization, Writing – review & editing. **Yong Li:** Funding acquisition, Project administration, Supervision, Writing – review & editing. **Tieying Hou:** Project administration, Supervision, Writing – review & editing.

Declaration of competing interest

The authors declare that they have no known competing financial interests or personal relationships that could have appeared to influence the work reported in this paper.

Acknowledgments

The authors would like to thank TCGA (<http://cancergenome.nih.gov>) for gene expression and survival information collection. Especially, we sincerely thank Prof. You Lang Zhou from Affiliated Hospital of Nantong University for analysis advice and helpful discussions.

Abbreviations

| | |
|--------------|--|
| CRC | colorectal cancer |
| TME | Tumor microenvironment |
| EMT | Epithelial-mesenchymal transition |
| PFS | Progression-free survival |
| Fges | Functional gene expression signatures |
| HLA | Human leukocyte antigen |
| TCGA | The Cancer Genome Atlas |
| GSVA | Gene set variation analysis |
| ssGSEA | Single-sample gene-set enrichment analysis |
| GDSC | Genomics of Drug Sensitivity in Cancer |
| qRT-PCR | Quantitative real-time PCR |
| TGF- β | Transforming growth factor beta |
| TMB | Tumor mutation burden |

Appendix A. Supplementary data

Supplementary data to this article can be found online at <https://doi.org/10.1016/j.heliyon.2023.e21346>.

References

- [1] L.H. Biller, D. Schrag, Diagnosis and treatment of metastatic colorectal cancer: a review, *JAMA* 325 (2021) 669–685, <https://doi.org/10.1001/jama.2021.0106>.
- [2] A.B. Benson, A.P. Venook, M.M. Al-Hawary, M.A. Arain, Y.-J. Chen, K.K. Ciombor, S. Cohen, H.S. Cooper, D. Deming, L. Farkas, I. Garrido-Laguna, J.L. Grem, A. Gunn, J.R. Hecht, S. Hoffe, J. Hubbard, S. Hunt, K.L. Johung, N. Kirilcuk, S. Krishnamurthi, W.A. Messersmith, J. Meyerhardt, E.D. Miller, M.F. Mulcahy, S. Nurkin, M.J. Overman, A. Parikh, H. Patel, K. Pedersen, L. Saltz, C. Schneider, D. Shibata, J.M. Skibber, C.T. Sofocleous, E.M. Stoffel, E. Stotsky-Himelfarb, C. G. Willett, K.M. Gregory, L.A. Gurski, Colon cancer, version 2.2021, NCCN clinical practice guidelines in oncology, *J. Natl. Compr. Cancer Netw.* 19 (2021) 329–359, <https://doi.org/10.6004/jnccn.2021.0012>.
- [3] T. Yoshino, D. Arnold, H. Taniguchi, G. Pentheroudakis, K. Yamazaki, R.-H. Xu, T.W. Kim, F. Ismail, I.B. Tan, K.-H. Yeh, A. Grothey, S. Zhang, J.B. Ahn, M. Y. Mastura, D. Chong, L.-T. Chen, S. Kopetz, T. Eguchi-Nakajima, H. Ebi, A. Ohtsu, A. Cervantes, K. Muro, J. Tabernero, H. Minami, F. Ciardiello, J.-Y. Douillard, Pan-Asian adapted ESMO consensus guidelines for the management of patients with metastatic colorectal cancer: a JSMO-ESMO initiative endorsed by CSCO, KACO, MOS, SSO and TOS, *Ann. Oncol.* 29 (2018) 44–70, <https://doi.org/10.1093/annonc/mdx738>.
- [4] N. Shah, S. Sukumar, The Hox genes and their roles in oncogenesis, *Nat. Rev. Cancer* 10 (2010) 361–371, <https://doi.org/10.1038/nrc2826>.
- [5] M. Mallo, Reassessing the role of hox genes during vertebrate development and evolution, *Trends Genet.* 34 (2018) 209–217, <https://doi.org/10.1016/j.tig.2017.11.007>.
- [6] S. Yang, J.-Y. Lee, H. Hur, J.H. Oh, M.H. Kim, Up-regulation of HOXB cluster genes are epigenetically regulated in tamoxifen-resistant MCF7 breast cancer cells, *BMB Rep* 51 (2018) 450–455, <https://doi.org/10.5483/bmbrep.2018.51.9.020>.
- [7] M.C. Errico, K. Jin, S. Sukumar, A. Carè, The widening sphere of influence of HOXB7 in solid tumors, *Cancer Res.* 76 (2016) 2857–2862, <https://doi.org/10.1158/0008-5472.CAN-15-3444>.
- [8] J. Su, Y.-H. Huang, X. Cui, X. Wang, X. Zhang, Y. Lei, J. Xu, X. Lin, K. Chen, J. Lv, M.A. Goodell, W. Li, Homeobox oncogene activation by pan-cancer DNA hypermethylation, *Genome Biol.* 19 (2018) 108, <https://doi.org/10.1186/s13059-018-1492-3>.
- [9] S.A. de Bessa Garcia, M. Araújo, T. Pereira, J. Mouta, R. Freitas, HOX genes function in Breast Cancer development, *Biochim Biophys Acta Rev Cancer.* 1873 (2020), 188358, <https://doi.org/10.1016/j.bbcan.2020.188358>.
- [10] S. Kamalakaran, V. Varadan, H.E. Giercksky Russnes, D. Levy, J. Kendall, A. Janevski, M. Riggs, N. Banerjee, M. Synnestevedt, E. Schlichting, R. Kåresen, K. Shama Prasada, H. Rotti, R. Rao, L. Rao, M.-H. Eric Tang, K. Satyamoorthy, R. Lucito, M. Wigler, N. Dimitrova, B. Naume, A.-L. Borresen-Dale, J.B. Hicks, DNA methylation patterns in luminal breast cancers differ from non-luminal subtypes and can identify relapse risk independent of other clinical variables, *Mol. Oncol.* 5 (2011) 77–92, <https://doi.org/10.1016/j.molonc.2010.11.002>.
- [11] H. Lei, H. Wang, A.H. Juan, F.H. Ruddle, The identification of Hoxc8 target genes, *Proc. Natl. Acad. Sci. U. S. A.* 102 (2005) 2420–2424, <https://doi.org/10.1073/pnas.0409700102>.
- [12] C. Gong, J. Zou, M. Zhang, J. Zhang, S. Xu, S. Zhu, M. Yang, D. Li, Y. Wang, J. Shi, Y. Li, Upregulation of MGP by HOXC8 promotes the proliferation, migration, and EMT processes of triple-negative breast cancer, *Mol. Carcinog.* 58 (2019) 1863–1875, <https://doi.org/10.1002/mc.23079>.
- [13] S.D. Axlund, J.R. Lambert, S.K. Nordeen, HOXC8 inhibits androgen receptor signaling in human prostate cancer cells by inhibiting SRC-3 recruitment to direct androgen target genes, *Mol. Cancer Res.* 8 (2010) 1643–1655, <https://doi.org/10.1158/1541-7786.MCR-10-0111>.
- [14] Y. Alami, V. Castronovo, D. Belotti, D. Flagiello, N. Clause, HOXC5 and HOXC8 expression are selectively turned on in human cervical cancer cells compared to normal keratinocytes, *Biochem. Biophys. Res. Commun.* 257 (1999) 738–745, <https://doi.org/10.1006/bbrc.1999.0516>.

- [15] H. Liu, M. Zhang, S. Xu, J. Zhang, J. Zou, C. Yang, Y. Zhang, C. Gong, Y. Kai, Y. Li, HOXC8 promotes proliferation and migration through transcriptional up-regulation of TGF β 1 in non-small cell lung cancer, *Oncogenesis* 7 (2018) 1, <https://doi.org/10.1038/s41389-017-0016-4>.
- [16] S.K. Wculek, I. Malanchi, Neutrophils support lung colonization of metastasis-initiating breast cancer cells, *Nature* 528 (2015) 413–417, <https://doi.org/10.1038/nature16140>.
- [17] R.N. Hanna, C. Cekic, D. Sag, R. Tacke, G.D. Thomas, H. Nowyhed, E. Herrley, N. Rasquinha, S. McArdle, R. Wu, E. Peluso, D. Metzger, H. Ichinose, I. Shaked, G. Chodaczek, S.K. Biswas, C.C. Hedrick, Patrolling monocytes control tumor metastasis to the lung, *Science* 350 (2015) 985–990, <https://doi.org/10.1126/science.aac9407>.
- [18] S. Hänzelmann, R. Castelo, J. Guinney, GSEA: gene set variation analysis for microarray and RNA-seq data, *BMC Bioinf.* 14 (2013) 7, <https://doi.org/10.1186/1471-2105-14-7>.
- [19] N. Auslander, G. Zhang, J.S. Lee, D.T. Frederick, B. Miao, T. Moll, T. Tian, Z. Wei, S. Madan, R.J. Sullivan, G. Boland, K. Flaherty, M. Herlyn, E. Ruppin, Robust prediction of response to immune checkpoint blockade therapy in metastatic melanoma, *Nat. Med.* 24 (2018) 1545–1549, <https://doi.org/10.1038/s41591-018-0157-9>.
- [20] V. Thorsson, D.L. Gibbs, S.D. Brown, D. Wolf, D.S. Bortone, T.-H. Ou Yang, E. Porta-Pardo, G.F. Gao, C.L. Plaisier, J.A. Eddy, E. Ziv, A.C. Culhane, E.O. Paull, I.K. A. Sivakumar, A.J. Gentles, R. Malhotra, F. Farshidfar, A. Colaprico, J.S. Parker, L.E. Mose, N.S. Vo, J. Liu, Y. Liu, J. Rader, V. Dhankani, S.M. Reynolds, R. Bowlby, A. Califano, A.D. Cherniack, D. Anastassiou, D. Bedognetti, Y. Mokrab, A.M. Newman, A. Rao, K. Chen, A. Krasnitz, H. Hu, T.M. Malta, H. Noushmehr, C.S. Peadarallu, S. Bullman, A.I. Ojesina, A. Lamb, W. Zhou, H. Shen, T.K. Choueiri, J.N. Weinstein, J. Guinney, J. Saltz, R.A. Holt, C.S. Rabkin, , Cancer Genome Atlas Research Network, A.J. Lazar, J.S. Serody, E.G. Demicco, M.L. Disis, B.G. Vincent, I. Shmulevich, The immune landscape of cancer, *Immunity* 48 (2018) 812–830.e14, <https://doi.org/10.1016/j.immuni.2018.03.023>.
- [21] K. Yoshihara, M. Shahmoradgoli, E. Martínez, R. Vegesna, H. Kim, W. Torres-Garcia, V. Treviño, H. Shen, P.W. Laird, D.A. Levine, S.L. Carter, G. Getz, K. Stenke-Hale, G.B. Mills, R.G.W. Verhaak, Inferring tumour purity and stromal and immune cell admixture from expression data, *Nat. Commun.* 4 (2013) 2612, <https://doi.org/10.1038/ncomms3612>.
- [22] D. Aran, Z. Hu, A.J. Butte, xCell: digitally portraying the tissue cellular heterogeneity landscape, *Genome Biol.* 18 (2017) 220, <https://doi.org/10.1186/s13059-017-1349-1>.
- [23] A. Bagaev, N. Kotlov, K. Nomie, V. Svekolkina, A. Gafurov, O. Isaeva, N. Osokin, I. Kozlov, F. Frenkel, O. Gancharova, N. Almog, M. Tsiper, R. Ataullakhanov, N. Fowler, Conserved pan-cancer microenvironment subtypes predict response to immunotherapy, *Cancer Cell* 39 (2021) 845–865.e7, <https://doi.org/10.1016/j.ccell.2021.04.014>.
- [24] V.D. Blondel, J.-L. Guillaume, R. Lambiotte, E. Lefebvre, Fast unfolding of communities in large networks, *J. Stat. Mech* 2008 (2008), P10008, <https://doi.org/10.1088/1742-5468/2008/10/P10008>.
- [25] A. Colaprico, T.C. Silva, C. Olsen, L. Garofano, C. Cava, D. Garolini, T.S. Sabedot, T.M. Malta, S.M. Pagnotta, I. Castiglioni, M. Ceccarelli, G. Bontempi, H. Noushmehr, TCGAbiolinks: an R/Bioconductor package for integrative analysis of TCGA data, *Nucleic Acids Res.* 44 (2016) e71, <https://doi.org/10.1093/nar/gkv1507>.
- [26] A. Mayakonda, D.-C. Lin, Y. Assenov, C. Plass, H.P. Koeffler, Maftools: efficient and comprehensive analysis of somatic variants in cancer, *Genome Res.* 28 (2018) 1747–1756, <https://doi.org/10.1101/gr.239244.118>.
- [27] D. Maeser, R.F. Gruener, R.S. Huang, oncoPredict: an R package for predicting in vivo or cancer patient drug response and biomarkers from cell line screening data, *Briefings Bioinf.* 22 (2021), <https://doi.org/10.1093/bib/bbab260>.
- [28] S. Göllner, T. Oellerich, S. Agrawal-Singh, T. Schenk, H.-U. Klein, C. Rohde, C. Pabst, T. Sauer, M. Lerdrup, S. Tavor, F. Stölzel, S. Herold, G. Ehninger, G. Köhler, K.-T. Pan, H. Urlaub, H. Serve, M. Dugas, K. Spiekermann, B. Vick, I. Jeremias, W.E. Berdel, K. Hansen, A. Zelent, C. Wickenhauser, L.P. Müller, C. Thiede, C. Müller-Tidow, Loss of the histone methyltransferase EZH2 induces resistance to multiple drugs in acute myeloid leukemia, *Nat. Med.* 23 (2017) 69–78, <https://doi.org/10.1038/nm.4247>.
- [29] S. Mariathasan, S.J. Turley, D. Nickles, A. Castiglioni, K. Yuen, Y. Wang, E.E. Kadel, H. Koeppen, J.L. Astarita, R. Cubas, S. Jhunjhunwala, R. Banchereau, Y. Yang, Y. Guan, C. Chalouni, J. Zhai, Y. Şenbabaoglu, S. Santoro, D. Sheinson, J. Hung, J.M. Giltman, A.A. Pierce, K. Mesh, S. Lianoglou, J. Riegler, R.A. D. Carano, P. Eriksson, M. Höglund, L. Somarriva, D.L. Halligan, M.S. van der Heijden, Y. Loriot, J.E. Rosenberg, L. Fong, I. Mellman, D.S. Chen, M. Green, C. Derleth, G.D. Fine, P.S. Hegde, R. Bourgon, T. Powles, TGF β attenuates tumour response to PD-L1 blockade by contributing to exclusion of T cells, *Nature* 554 (2018) 544–548, <https://doi.org/10.1038/nature25501>.
- [30] D.V.F. Tauriello, S. Palomo-Ponce, D. Stork, A. Berenguer-Llgero, J. Badia-Ramentol, M. Iglesias, M. Sevillano, S. Ibiza, A. Cañellas, X. Hernando-Mombona, D. Byrom, J.A. Matarin, A. Calon, E.I. Rivas, A.R. Nebreda, A. Riera, C.S.-O. Attolini, E. Batlle, TGF β drives immune evasion in genetically reconstituted colon cancer metastasis, *Nature* 554 (2018) 538–543, <https://doi.org/10.1038/nature25492>.
- [31] X. Sun, B. Wu, H.-C. Chiang, H. Deng, X. Zhang, W. Xiong, J. Liu, A.M. Rozeboom, B.T. Harris, E. Blommaert, A. Gomez, R.E. Garcia, Y. Zhou, P. Mitra, M. Prevost, D. Zhang, D. Banik, C. Isaacs, D. Berry, C. Lai, K. Chaldekis, P.S. Latham, C.A. Brantner, A. Popratiloff, V.X. Jin, N. Zhang, Y. Hu, M.A. Pujana, T. J. Curriel, Z. An, R. Li, Tumour DDR1 promotes collagen fibre alignment to instigate immune exclusion, *Nature* 599 (2021) 673–678, <https://doi.org/10.1038/s41586-021-04057-2>.
- [32] J.J. Luke, R. Bao, R.F. Sweis, S. Spranger, T.F. Gajewski, WNT/ β -catenin pathway activation correlates with immune exclusion across human cancers, *Clin. Cancer Res.* 25 (2019) 3074–3083, <https://doi.org/10.1158/1078-0432.CCR-18-1942>.
- [33] S. Spranger, R. Bao, T.F. Gajewski, Melanoma-intrinsic β -catenin signalling prevents anti-tumour immunity, *Nature* 523 (2015) 231–235, <https://doi.org/10.1038/nature14404>.
- [34] D.M.W. Zaiss, W.C. Gause, L.C. Osborne, D. Artis, Emerging functions of amphiregulin in orchestrating immunity, inflammation, and tissue repair, *Immunity* 42 (2015) 216–226, <https://doi.org/10.1016/j.immuni.2015.01.020>.
- [35] Q. Xu, Q. Long, D. Zhu, D. Fu, B. Zhang, L. Han, M. Qian, J. Guo, J. Xu, L. Cao, Y.E. Chin, J.-P. Coppé, E.W.-F. Lam, J. Campisi, Y. Sun, Targeting amphiregulin (AREG) derived from senescent stromal cells diminishes cancer resistance and averts programmed cell death 1 ligand (PD-L1)-mediated immunosuppression, *Aging Cell* 18 (2019), e13027, <https://doi.org/10.1111/acer.13027>.
- [36] Z. Chen, J. Chen, Y. Gu, C. Hu, J.-L. Li, S. Lin, H. Shen, C. Cao, R. Gao, J. Li, P.K. Ha, F.J. Kaye, J.D. Griffin, L. Wu, Aberrantly activated AREG-EGFR signaling is required for the growth and survival of CRTCl-MAML2 fusion-positive mucoepidermoid carcinoma cells, *Oncogene* 33 (2014) 3869–3877, <https://doi.org/10.1038/onc.2013.348>.
- [37] M. G. H. Ba, S. P. W. Ja, Hallmarks of response, resistance, and toxicity to immune checkpoint blockade, *Cell* 184 (2021), <https://doi.org/10.1016/j.cell.2021.09.020>.
- [38] H. Ps, K.V. E.S. The where, the when, and the How of Immune Monitoring for Cancer Immunotherapies in the Era of Checkpoint Inhibition, *Clinical Cancer Research : An Official Journal of the American Association for Cancer Research*, 2016, <https://doi.org/10.1158/1078-0432.CCR-15-1507>, 22.
- [39] H. Rs, S. Jc, K. Mf, F. Gd, H. O, G. Ms, S. Ja, M. Df, P. Jd, G. Sn, K. He, H. L, L. Dp, R. S, L. M, X. Y, M.A. K. H, H. Ps, M. I, C. Ds, H. Fs, Predictive correlates of response to the anti-PD-L1 antibody MPDL3280A in cancer patients, *Nature* 515 (2014), <https://doi.org/10.1038/nature14011>.
- [40] T. J. S. A, H.-L. Vm, Comprehensive analysis of the clinical immuno-oncology landscape, *Ann. Oncol. : Official Journal of the European Society for Medical Oncology* 29 (2018), <https://doi.org/10.1093/annonc/mdx755>.
- [41] J.D. Wolchok, V. Chiarion-Sileni, R. Gonzalez, P. Rutkowski, J.-J. Grob, C.L. Cowey, C.D. Lao, J. Wagstaff, D. Schadendorf, P.F. Ferrucci, M. Smylie, R. Dummer, A. Hill, D. Hogg, J. Haanen, M.S. Carlino, O. Bechter, M. Maio, I. Marquez-Rodas, M. Guidoboni, G. McArthur, C. Lebbé, P.A. Ascierto, G.V. Long, J. Cebon, J. Sosman, M.A. Postow, M.K. Callahan, D. Walker, L. Rollin, R. Bshore, F.S. Hodi, J. Larkin, Overall survival with combined nivolumab and ipilimumab in advanced melanoma, *N. Engl. J. Med.* 377 (2017) 1345–1356, <https://doi.org/10.1056/NEJMoa1709684>.
- [42] Y. Owada-Ozaki, S. Muto, H. Takagi, T. Inoue, Y. Watanabe, M. Fukuhara, T. Yamaura, N. Okabe, Y. Matsumura, T. Hasegawa, J. Ohsugi, M. Hoshino, Y. Shio, H. Nanamiya, J.-I. Imai, T. Isogai, S. Watanabe, H. Suzuki, Prognostic impact of tumor mutation burden in patients with completely resected non-small cell lung cancer: brief report, *J. Thorac. Oncol.* 13 (2018) 1217–1221, <https://doi.org/10.1016/j.jtho.2018.04.003>.

- [43] H. Adwan, M. Zhivkova-Galunsk, R. Georges, E. Eyol, J. Kleeff, N.A. Giese, H. Friess, F. Bergmann, M.R. Berger, Expression of HOXC8 is inversely related to the progression and metastasis of pancreatic ductal adenocarcinoma, *Br. J. Cancer* 105 (2011) 288–295, <https://doi.org/10.1038/bjc.2011.217>.
- [44] Y. Li, M. Zhang, H. Chen, Z. Dong, V. Ganapathy, M. Thangaraju, S. Huang, Ratio of miR-196s to HOXC8 messenger RNA correlates with breast cancer cell migration and metastasis, *Cancer Res.* 70 (2010) 7894–7904, <https://doi.org/10.1158/0008-5472.CAN-10-1675>.
- [45] Y. Jiang, Z. Wang, C. Ying, J. Hu, T. Zeng, L. Gao, FMR1/circCHAF1A/miR-211-5p/HOXC8 feedback loop regulates proliferation and tumorigenesis via MDM2-dependent p53 signaling in GSCs, *Oncogene* 40 (2021) 4094–4110, <https://doi.org/10.1038/s41388-021-01833-2>.
- [46] F. Di Nicolantonio, P.P. Vitiello, S. Marsoni, S. Siena, J. Tabernero, L. Trusolino, R. Bernards, A. Bardelli, Precision oncology in metastatic colorectal cancer - from biology to medicine, *Nat. Rev. Clin. Oncol.* 18 (2021) 506–525, <https://doi.org/10.1038/s41571-021-00495-z>.
- [47] P. Xu, X. Zhang, W. Ni, H. Fan, J. Xu, Y. Chen, J. Zhu, X. Gu, L. Yang, R. Ni, B. Chen, W. Shi, Upregulated HOXC8 expression is associated with poor prognosis and oxaliplatin resistance in hepatocellular carcinoma, *Dig. Dis. Sci.* 60 (2015) 3351–3363, <https://doi.org/10.1007/s10620-015-3774-x>.
- [48] M. Li, J. Cai, X. Han, Y. Ren, Downregulation of circNRIP1 suppresses the paclitaxel resistance of ovarian cancer via regulating the miR-211-5p/HOXC8 Axis, *Cancer Manag. Res.* 12 (2020) 9159–9171, <https://doi.org/10.2147/CMAR.S268872>.
- [49] J. Cooney, Expansion of cord blood stem cells and enhancing their mobilization and homing potential using mesenchymal stromal cells, *Blood* 132 (2018) 3344, <https://doi.org/10.1182/blood-2018-99-117779>.
- [50] H. Su, G. Fan, J. Huang, X. Qiu, LncRNA HOXC-AS3 promotes non-small-cell lung cancer growth and metastasis through upregulation of YBX1, *Cell Death Dis.* 13 (2022) 307, <https://doi.org/10.1038/s41419-022-04723-x>.
- [51] D.P. Carbone, M. Reck, L. Paz-Ares, B. Creelan, L. Horn, M. Steins, E. Felip, M.M. van den Heuvel, T.-E. Ciuleanu, F. Badin, N. Ready, T.J.N. Hiltermann, S. Nair, R. Jurgens, S. Peters, E. Minenza, J.M. Wrangle, D. Rodriguez-Abreu, H. Borghaei, G.R. Blumenschein, L.C. Villaruz, L. Havel, J. Krejci, J. Corral Jaime, H. Chang, W.J. Geese, P. Bhagavatheswaran, A.C. Chen, M.A. Socinski, CheckMate 026 investigators, first-line nivolumab in stage IV or recurrent non-small-cell lung cancer, *N. Engl. J. Med.* 376 (2017) 2415–2426, <https://doi.org/10.1056/NEJMoa1613493>.